Controlling the Location of Bare Nanoparticles in Polymer-Nanoparticle Blend Films by Adding Polymer-Grafted Nanoparticles

Kishore Kumar Sriramoju and Venkat Padmanabhan*

Department of Chemical Engineering, Indian Institute of Technology (IIT), Kharagpur, West Bengal 721302, India

(Received 26 January 2015; revised manuscript received 16 April 2015; published 24 June 2015)

We present molecular dynamics simulations of polymer-nanoparticle blends in films containing both grafted and ungrafted nanoparticles where the particle cores are identical and grafted chains are similar to a matrix polymer. Our results indicate that it is possible to control the location of bare nanoparticles in the film by adding small amounts of polymer-grafted nanoparticles. In the presence of a substrate, bare particles are entropically pushed to the surface. We observed that the introduction of grafted particles to the blend prevents the migration of bare particles to the surface. This unusual behavior is caused by the formation of binary aspherical clusters due to the presence of grafted particles. Hence, parameters including grafting density and the length of the grafted polymer play a significant role in dictating the spatial arrangement of bare particles in the blend film. At higher values of these parameters, the grafted particle core is shielded from depletion attractions causing the density of bare particles to increase back near the surface.

DOI: 10.1103/PhysRevLett.114.258301 PACS numbers: 82.35.Np, 36.20.Ey, 36.20.Fz, 65.40.gd

Polymer nanocomposites are an important class of materials that have received significant interest in the past few decades due to their unique set of properties that are far superior to those of pristine polymers [1–5]. However, a precise morphology of nanoparticles is required in the matrix for specific macroscopic property enhancement [6–11]. It is believed that a good dispersion of nanoparticles in polymer matrices is extremely difficult to achieve as inorganic fillers are often immiscible with the organic phase [5,12,13]. One of the most successful techniques that has been widely used to control the spatial arrangement of nanoparticles in a polymer matrix is to shield the particle from depletion attraction by grafting its surface with chains that are chemical similar to the matrix polymer [4,14–20]. Theoretical and experimental work on polymer-grafted nanoparticles have shown that the interparticle interactions can be tuned by appropriately choosing the right set of parameters, including graft molecular weight, density, polydispersity, and stiffness [21–27].

Although all of the studies cited above have given significant insights into effective interactions and the phase behavior of polymer-nanoparticle blends, most of them pertain to "bulk" conditions. In contrast, a number of contexts, such as chemical sensors, dielectric coatings, membranes for fuel cells, etc., involve polymer-particle blends in confined films where the influence of external substrates cannot be ignored. Several experimental and theoretical studies have shown that nanoparticles migrate to the air-substrate interface upon annealing [9,28–36]. In these systems, the self-assembly is controlled by the interplay between contributions from surface energies, dispersion forces, and entropy to the total free energy of the system [8,28,35,37,38]. Such a behavior can be advantageous or disadvantageous depending on the nature of application. For instance, utilization of this behavior has led to the development of self-healing materials [8,9,39]. In organic solar cells, the segregation of nanoparticles to the bottom electrode is advantageous as it facilitates efficient transfer of electrons to the electrode. Conversely, segregation to the top electrode is disadvantageous as it blocks sunlight from entering the active layer [40,41].

Earlier studies on blends of polymers and nanoparticles have suggested that the presence of an interface has a profound impact on the final morphology of constituents within the film [7,16,33,34,42–45]. Theoretical studies on athermal blends have indicated a first-order phase transition of nanoparticle migration to the substrate [35]. In such blends (e.g., polystyrene nanoparticles in polystyrene matrix), where interactions in the blend are predominately entropic because of the chemical similarity of nanoparticles and polymer, the migration of nanoparticles to the substrate is driven by purely entropic forces [32,33]. This tendency of nanoparticles to migrate to the substrate was shown to decrease with the increase in strength of polymer-substrate attraction, chain stiffness [28,46], and by grafting the particle surface with chains that are similar to a matrix polymer [47].

While all these techniques could be used as guides for synthesis of materials where a strong control over the morphology is essential, often it is not feasible to modify the polymer or the nanoparticle to achieve this level of control. In such cases, it becomes extremely important to devise strategies to control the morphology without directly modifying the constituents. In this Letter, we present MD simulations of polymer-nanoparticle blends in films. Two types of nanoparticles were considered in each system: one bare and the other with chains grafted onto its surface. The particle cores in both types were identical and spherical. We observed that by adding certain amounts of grafted particles

to the blend the location of bare particles could be significantly controlled. Our simulations suggest that to gain control over the spatial arrangement of nanoparticles in polymer films, one need not modify the particles directly, in contrast to the current notion. This provides an advantage of retaining the specific property of nanoparticles that may be lost due to grafting.

We modeled brush and matrix polymers as coarse grained bead-spring chains, using the finite extensible nonlinear elastic potential with standard values [48]. All monomers were chemically identical with mass m and diameter σ. The degree of polymerization for matrix chains, $M_m = 40$, was chosen so that the chains exhibit a polymerlike behavior. Nanoparticles were represented as uniform spheres of mass m and diameter $\sigma_n = 4\sigma$. Polymer-grafted nanoparticles were constructed by uniformly grafting polymer chains onto the surface of each nanoparticle. In this study the grafting density (Σ_g) was varied from 0 to 0.36 chains/σ^2 and the graft length (M_g) from 5 to 25 beads. We modeled a purely athermal system where all beads interact via the Weeks-Chanler-Andersen potential [49]. The walls were modeled as massless boundaries with bead-wall interactions set as purely repulsive. The number of matrix chains N_m and nanoparticles N_n (bare + grafted) were chosen such that the total packing fraction $\eta_T = (\pi/6)(\rho_p\sigma_p^3 + \rho_n\sigma_n^3 + \rho_g\sigma_g^3)$ and bare-particle volume fraction $\phi_b = \rho_b\sigma_n^3/(\rho_p\sigma_p^3 + \rho_n\sigma_n^3 + \rho_g\sigma_g^3)$ were kept constant at 0.415 (which corresponds to a meltlike condition) and 0.10, respectively. Here, the subscript n corresponds to both bare and grafted particle cores and b corresponds to only bare particles. The compositions of all systems with varying concentrations of grafted particles are given in Table I. A temperature of $T = 1.0$ was maintained using a Nose-Hoover thermostat with a damping parameter of 0.01. Each system was equilibrated for 10^7 MD steps with a $\delta t = 0.003$ and the data for postprocessing were collected every 10 000 steps from subsequent production runs of an additional 2×10^6 MD steps. Additional details of the simulation methods are presented in Supplemental Material [50].

We first study the effect of grafting parameters including Σ_g and M_g on segregation of nanoparticles to the substrate

TABLE I. Individual volume fractions of bare (ϕ_b) and grafted nanoparticles (ϕ_g), total volume fraction (ϕ_T), and total packing fraction (η_T) of systems with different fractions of grafted nanoparticles (GNP).

S. No.	% of GNP	ϕ_b	ϕ_g	ϕ_T	η_T
1	0	0.1	0.0000	0.1000	0.415
2	10	0.1	0.0111	0.1111	0.415
3	20	0.1	0.0247	0.1247	0.415
4	30	0.1	0.0427	0.1427	0.415
5	40	0.1	0.0666	0.1666	0.415
6	50	0.05	0.05	0.1000	0.415

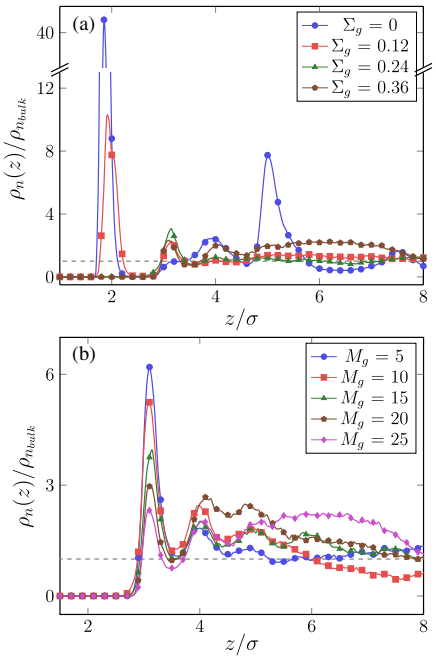

FIG. 1 (color online). Nanoparticle density profiles perpendicular to the surface for various (a) grafting densities, with $M_g = 25$, and (b) grafted chain length, with $\Sigma_g = 0.36$, in systems with homogeneous particles. All particles are either grafted or ungrafted.

in systems where all nanoparticles were either grafted or ungrafted ($M_g = 0$). Figure 1 shows the density profiles of nanoparticles perpendicular to the surface for various Σ_g, with $M_g = 25$ [Fig. 1(a)], and M_g, with $\Sigma_g = 0.36$ [Fig. 1(b)]. As expected, the density profile for the bare-particle system ($\Sigma_g = 0$) shows the highest peak near the surface and the peak height decreases as we increase both Σ_g and M_g. In Fig. 1(a), we also note that as the grafting density increases, the first peak in the density profiles shifts to higher values of z. In athermal blends, in the presence of a substrate, the polymer chains increase their configurational entropy by pushing nanoparticles to the surface. This "entropic push" is severe when the particles are bare and decreases when particles are grafted with polymer chains that are identical to a matrix polymer. This opposing force that arises from the increase in dispersibility of nanoparticles in a polymer matrix and loss in configurational entropy of grafted chains that are closer to the surface becomes stronger with the increase in grafting parameters, and beyond a certain limit, it becomes thermodynamically unfavorable for the polymers to push nanoparticles to the surface [16,47]. The density profiles for particles perpendicular to the surface with $\Sigma_g = 0.12$ and 0.24 are presented in Fig. S1 of SM [50].

Using the above technique, spatial arrangement of nanoparticles in polymer nanocomposites can be precisely controlled. However, it is required that the nanoparticle surface chemistry be altered in order to achieve such a level of control. Here, we report that it is indeed possible

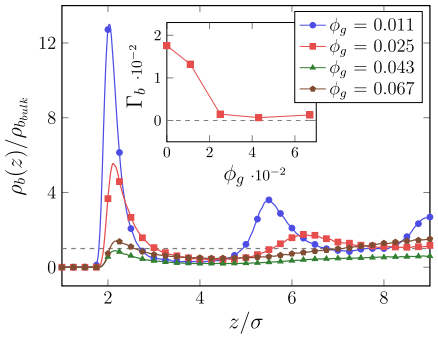

FIG. 2 (color online). Bare particle density profiles perpendicular to the surface for various concentrations of grafted particles ($\Sigma_g = 0.36$ and $M_g = 25$) in systems with a mixture of bare and grafted particles. Inset: Excess adsorption of bare particles on the surface as a function of volume fraction of grafted particles.

to control the location of nanoparticles in polymer-nanoparticle blend films without directly grafting the nanoparticles of interest with polymer chains. We achieve this by introducing additional particles to the polymer–bare-particle blend that are grafted with chains similar to the matrix polymer. Our results show that the location of bare particles could be controlled by changing the amount and properties of grafted particles. Figure 2 shows the density profiles of only bare particles perpendicular to the surface for varying concentrations of grafted particles with $\Sigma_g = 0.36$ and $M_g = 25$. It has recently been proposed that homogeneous dispersion of polymer-grafted nanoparticles in a polymer matrix is achieved when the graft length is greater than approximately $1/4$ the length of matrix chains [55]. So, Σ_g and M_g were chosen such that the grafted particles dispersed homogeneously in the bulk of the film at these conditions. As the concentration of grafted particles in the blend increases, the density of bare particles near the surface decreases. This can also be seen clearly in the inset of Fig. 2 that shows the excess adsorption (Γ_b) of bare particles on the surface. Here, excess adsorption is a measure of the concentration of (bare) particles near the surface relative to the bulk and is calculated as

$$\Gamma_b = \int_0^{L_z/2} dz[\rho_b(z) - \rho_{b_{\text{bulk}}}], \tag{1}$$

where, L_z is the box dimension perpendicular to the surface and ρ_b is the number density of bare nanoparticles. When the grafted particle concentration is 0, nanoparticles (bare) migrate to the surface as indicated by a positive value of Γ_b. As the concentration of grafted particles increases, Γ_b decreases, and for these sets of graft parameters, when the concentration of grafted particles reached a value of $\phi_g = 0.043$, $\Gamma_b \sim 0$, indicating that bare particles are no longer accumulated on the surface. We also note that even though the total concentration of nanoparticles (bare + grafted) increases with the addition of grafted

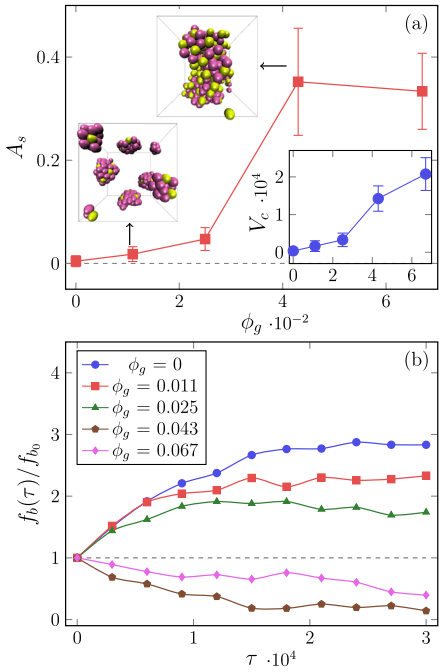

FIG. 3 (color online). (a) Asphericity of nanoparticle clusters formed within the system as a function of volume fraction of grafted particles ($\Sigma_g = 0.36$ and $M_g = 25$). Insets: Binary clusters (bare and grafted particles are represented by pink and green spheres, respectively) formed in the bulk for $\phi_g = 0.011$ (left), 0.043 (right) and average volume of clusters as a function of grafted particle concentration. (b) Normalized fraction of bare particles near the surface as a function of simulation time. Here, f_{b_0} is the fraction of bare particles near the surface in randomly generated initial configuration.

particles (Table I), the bare particles are pulled away from the surface. At these conditions, polymers become the major constituent near the surface (Fig. S2 of SM [50]). For still higher concentrations, the effect of grafting on segregation decreases, resulting in both bare and grafted particles migrating to the substrate.

Although the grafting density of polymer-grafted nanoparticles is relatively low, at low concentrations it is sufficient to shield the depletion attraction between two grafted particles. However, it is not sufficient to shield the depletion attraction between grafted and bare particles. This results in the formation of binary clusters with at least one layer of bare particles between any two grafted particles (Fig. S3 of SM [50]). At low concentrations of grafted particles, several isolated clusters form that are free to move toward the surface. When the concentration of grafted particles increases, the anisotropy of clusters also increases, resulting in the formation of binary clusters in the bulk that prevents the migration of bare particles to the surface. This can be seen clearly in Fig. 3(a) that shows the asphericity (A_s) of clusters as a function of grafted particle concentration. The calculation of cluster asphericity (A_s) is described in the SM [50]. In the inset of Fig. 3(a), we also show the average volume (V_c) of clusters as a function of ϕ_g.

For low concentrations, the clusters are predominantly formed by the bare particles, and as the system size is significantly large in these simulations, these spherical aggregates are isolated. But as the concentration of grafted particles increases, the formation of anisotropic structures causes the interdomain spacing of nanoparticles to decrease, resulting in the aggregation of smaller clusters giving rise to larger clusters. Figure 3(b) shows the normalized fraction of bare particles migrating to the surface as a function of time during equilibration. At low concentrations of grafted particles, the clusters migrate to the surface easily. As the concentration of grafted particles is increased, the fraction of particles migrating to the surface decreases. Surprisingly, at $\phi_g = 0.043$ and 0.067, the fraction decreases below its starting point, indicating that bare particles that were near the surface in a randomly generated initial configuration were pulled away from the surface during equilibration. To ensure that our systems are thoroughly equilibrated and the large binary cluster formed in the bulk is thermodynamically compatible with the polymer, we carried out an additional simulation of polymers with a single large particle of size (diameter 22σ) and grafting density ($\Sigma_g = 0.27$ chains$/\sigma^2$) equivalent to the corresponding mean values of the binary cluster. We observed that in the time frame of our simulation, the large grafted particle moves significantly in the x and y directions but prefers to remain away from walls in the z direction. The mean-squared displacement of the particle in directions parallel and perpendicular to the wall and the evolution of the particle trajectory in the z direction are presented in Fig. S4 of SM [50].

Next we discuss the effects of the grafting density and the length of grafted chains on bare particle migration to the surface. We observe that these two parameters have a profound effect on controlling the location of bare particles in the blends. Figure 4(a) shows the density profiles of bare particles perpendicular to the surface for varying grafting densities. At low Σ_g, the surface coverage of grafted particles is not sufficient to shield off the depletion attraction between them and the surface as a major portion of their core is exposed. This results in accumulation of grafted particles on the surface (Fig. S5 of SM [50]) along with bare particles. For higher grafting densities, provided the graft length is long enough to increase the dispersion of grafted particles in the matrix (which is true in this case), the density of bare particles near the wall decreases as a result of grafted particles moving to the bulk pulling bare particles along with them. Figure 4(b) shows the density profiles of bare particles with varying lengths of grafted chains for the highest grafting density ($\Sigma_g = 0.36$) studied in this work. At low graft length and high grafting density, grafted particles exhibit autophobic dewetting with matrix chains causing them to behave as particles with an effective size bigger than their core diameter. In such cases, as the dispersibility of particles in the matrix is low, the system tries to increase its entropy by pushing both bare and grafted particles to the surface or by phase separation in the bulk. As we increase the graft length, the dispersibility of grafted particles in the matrix also increases without much change in the depletion attraction between bare and grafted particles. This leads to bare particles forming clusters with grafted particles and moving away from the surface. At low Σ_g and M_g, grafted particles behave similarly to bare particles and have minimum effect on the migration of bare particles to the surface (Fig. S5 of SM [50]). The effects of Σ_g and M_g were qualitatively similar for a 50:50 composition of the blend (Figs. S6 and S7 of SM [50]).

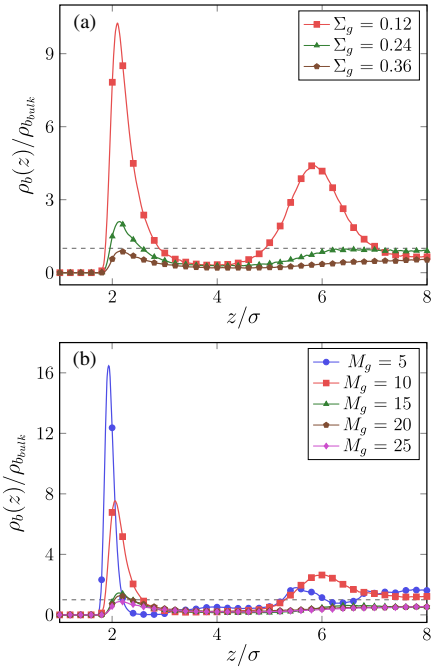

FIG. 4 (color online). Bare particle density profiles perpendicular to the surface for different (a) grafting densities, with $M_g = 25$, and (b) grafted chain length, with $\Sigma_g = 0.36$, in systems with $\phi_g = 0.043$.

In summary, this is one of the first studies that demonstrates the possibility of achieving thorough control over the location of bare nanoparticles in polymer nanocomposite films without modifying either the polymer or the nanoparticle of interest. The addition of grafted nanoparticles to athermal blends prevents the usual migration of bare particles to the surface upon annealing. Our observations indicate that a small amount of grafted particles is sufficient to pull all the bare particles away from the surface. These results suggest that it is not essential to follow the conventional approach of grafting nanoparticles to control the morphology of polymer nanocomposites and open new avenues to the design and development of advanced functional materials with enhanced properties.

We acknowledge the Department of Chemical Engineering at IIT Kharagpur for supporting this work and HPCC at Texas Tech University for providing computational facilities.

*Corresponding author.
venkatp@che.iitkgp.ernet.in

[1] K. Yoshimoto, T. S. Jain, K. V. Workum, P. F. Nealey, and J. J. de Pablo, Mechanical Heterogeneities in Model Polymer Glasses at Small Length Scales, Phys. Rev. Lett. **93**, 175501 (2004).
[2] B. J. Ash, R. W. Siegel, and L. S. Schadler, Mechanical behavior of alumina/poly(methyl methacrylate) nanocomposites, Macromolecules **37**, 1358 (2004).
[3] P. H. T. Vollenberg and D. Heikens, Particle size dependence of the Young's modulus of filled polymers: 1. Preliminary experiments, Polymer **30**, 1656 (1989).
[4] S. E. Harton and S. K. Kumar, Mean-field theoretical analysis of brush-coated nanoparticle dispersion in polymer matrices, J. Polym. Sci. B **46**, 351 (2008).
[5] M. E. Mackay, A. Tuteja, P. M. Duxbury, C. J. Hawker, B. Van Horn, Z. Guan, G. Chen, and R. S. Krishnan, General strategies for nanoparticle dispersion, Science **311**, 1740 (2006).
[6] P. Vettiger, G. Cross, M. Despont, U. Drechsler, U. Durig, B. Gotsmann, W. Haberle, M. A. Lantz, H. E. Rothuizen, R. Stutz, and G. K. Binnig, The "millipede"-nanotechnology entering data storage, IEEE Trans. Nanotechnol. **1**, 39 (2002).
[7] M. A. Holmes, M. E. Mackay, and R. K. Giunta, Nanoparticles for dewetting suppression of thin polymer films used in chemical sensors, J. Nanopart. Res. **9**, 753 (2007).
[8] S. Gupta, Q. Zhang, T. Emrick, A. C. Balazs, and T. P. Russell, Entropy-driven segregation of nanoparticles to cracks in multilayered composite polymer structures, Nat. Mater. **5**, 229 (2006).
[9] A. C. Balazs, T. Emrick, and T. P. Russell, Nanoparticle polymer composites: Where two small worlds meet, Science **314**, 1107 (2006).
[10] K. M. Coakley and M. D. McGehee, Conjugated polymer photovoltaic cells, Chem. Mater. **16**, 4533 (2004).
[11] V. Padmanabhan, Percolation of high-density polymer regions in nanocomposites: The underlying property for mechanical reinforcement, J. Chem. Phys. **139**, 144904 (2013).
[12] R. Krishnamoorti, Strategies for dispersing nanoparticles in polymers, MRS Bull. **32**, 341 (2007).
[13] A. Bansal, H. Yang, C. Li, K. Cho, B. C. Benicewicz, S. K. Kumar, and L. S. Schadler, Quantitative equivalence between polymer nanocomposites and thin polymer films, Nat. Mater. **4**, 693 (2005).
[14] D. Meng, S. K. Kumar, J. M. D. Lane, and G. S. Grest, Effective interactions between grafted nanoparticles in a polymer matrix, Soft Matter **8**, 5002 (2012).
[15] D. M. Trombly and V. Ganesan, Curvature effects upon interactions of polymer-grafted nanoparticles in chemically identical polymer matrices, J. Chem. Phys. **133**, 154904 (2010).
[16] P. F. Green, The structure of chain end-grafted nanoparticle/homopolymer nanocomposites, Soft Matter **7**, 7914 (2011).
[17] V. Goel, J. Pietrasik, H. Dong, J. Sharma, K. Matyjaszewski, and R. Krishnamoorti, Structure of polymer tethered highly grafted nanoparticles, Macromolecules **44**, 8129 (2011).
[18] D. L. Green and J. Mewis, Connecting the wetting and rheological behaviors of poly(dimethylsiloxane)-grafted silica spheres in poly(dimethylsiloxane) melts, Langmuir **22**, 9546 (2006).
[19] A. Bansal, H. Yang, C. Li, B. C. Benicewicz, S. K. Kumar, and L. S. Schadler, Controlling the thermomechanical properties of polymer nanocomposites by tailoring the polymer-particle interface, J. Polym. Sci. B **44**, 2944 (2006).
[20] C. K. Wu, K. L. Hultman, S. O'Brien, and J. T. Koberstein, Functional oligomers for the control and fixation of spatial organization in nanoparticle assemblies, J. Am. Chem. Soc. **130**, 3516 (2008).
[21] B. Palli and V. Padmanabhan, Chain flexibility for tuning effective interactions in blends of polymers and polymer-grafted nanoparticles, Soft Matter **10**, 6777 (2014).
[22] V. Pryamtisyn, V. Ganesan, A. Z. Panagiotopoulos, H. Liu, and S. K. Kumar, Modeling the anisotropic self-assembly of spherical polymer-grafted nanoparticles, J. Chem. Phys. **131**, 221102 (2009).
[23] P. Akcora, H. Liu, S. K. Kumar, J. Moll, Y. Li, B. C. Benicewicz, L. S. Schadler, D. Acehan, A. Z. Panagiotopoulos, V. Pryamtisyn, R. H. Colby, V. Ganesan, J. Ilavsky, P. Thiyagarajan, and J. F. Douglas, Anisotropic self-assembly of spherical polymer-grafted nanoparticles, Nat. Mater. **8**, 354 (2009).
[24] Q. Lan, L. F. Francis, and F. S. Bates, Silica nanoparticle dispersions in homopolymer versus block copolymer, J. Polym. Sci. B **45**, 2284 (2007).
[25] K. T. Marla and J. C. Meredith, Simulation of interaction forces between nanoparticles: end-grafted polymer modifiers, J. Chem. Theory Comput. **2**, 1624 (2006).
[26] B. J. Kim, J. Bang, C. J. Hawker, and E. J. Kramer, Effect of areal chain density on the location of polymer-modified gold nanoparticles in a block copolymer template, Macromolecules **39**, 4108 (2006).
[27] M. K. Corbierre, N. S. Cameron, M. Sutton, K. Laaziri, and R. B. Lennox, Gold nanoparticle/polymer nanocomposites: Dispersion of nanoparticles as a function of capping agent molecular weight and grafting density, Langmuir **21**, 6063 (2005).
[28] A. L. Frischknecht, V. Padmanabhan, and M. E. Mackay, Surface-induced phase behavior of polymer/nanoparticle blends with attractions, J. Chem. Phys. **136**, 164904 (2012).
[29] K. A. Barnes, J. F. Douglas, D. W. Liu, and A. Karim, Influence of nanoparticles and polymer branching on the dewetting of polymer films, Adv. Colloid Interface Sci. **94**, 83 (2001).
[30] M. E. Mackay, Y. Hong, M. Jeong, S. Hong, T. P. Russell, C. J. Hawker, R. Vestberg, and J. F. Douglas, Influence of dendrimer additives on the dewetting of thin polystyrene films, Langmuir **18**, 1877 (2002).
[31] R. S. Krishnan, M. E. Mackay, C. J. Hawker, and B. Van Horn, Influence of molecular architecture on the dewetting of thin polystyrene films, Langmuir **21**, 5770 (2005).
[32] R. S. Krishnan, M. E. Mackay, P. M. Duxbury, C. J. Hawker, S. Asokan, M. S. Wong, R. Goyette, and P. Thiyagarajan, Improved polymer thin-film wetting behavior through nanoparticle segregation to interfaces, J. Phys. Condens. Matter **19**, 356003 (2007).

[33] R. S. Krishnan, M. E. Mackay, P. M. Duxbury, M. Phillip, A. Pastor, C. J. Hawker, B. Van Horn, S. Asokan, and M. S. Wong, Self-assembled multilayers of nanocomponents, Nano Lett. **7**, 484 (2007).

[34] A. K. Barnes, A. Karim, J. F. Douglas, A. I. Nakatani, H. Gruell, and E. J. Amis, Suppression of dewetting in nanoparticle-filled polymer films, Macromolecules **33**, 4177 (2000).

[35] E. S. McGarrity, A. L. Frischknecht, L. J. D. Frink, and M. E. Mackay, Surface-Induced First-Order Transition in Athermal Polymer-Nanoparticle Blends, Phys. Rev. Lett. **99**, 238302 (2007).

[36] J. Y. Lee, Z. Shou, and A. C. Balazs, Predicting the morphologies of confined copolymer/nanoparticle mixtures, Macromolecules **36**, 7730 (2003).

[37] E. S. McGarrity, P. M. Duxbury, M. E. Mackay, and A. L. Frischknecht, Calculation of entropic terms governing nanoparticle self-assembly in polymer films, Macromolecules **41**, 5952 (2008).

[38] E. S. McGarrity, A. L. Frischknecht, and M. E. Mackay, Phase behavior of polymer/nanoparticle blends near a substrate, J. Chem. Phys. **128**, 154904 (2008).

[39] A. Alexeev, R. Verberg, and A. C. Balazs, Modeling the motion of microcapsules on compliant polymeric surfaces, Macromolecules **38**, 10244 (2005).

[40] C. C. Chang, C. F. Lin, J. M. Chiou, T. H. Ho, Y. Tai, J. H. Lee, Y. F. Chen, J. K. Wang, L. C. Chen, and K. H. Chen, Effects of cathode buffer layers on the efficiency of bulk-heterojunction solar cells, Appl. Phys. Lett. **96**, 263506 (2010).

[41] J. H. Seo, A. Gutacker, Y. Sun, H. Wu, F. Huang, Y. Cao, U. Scherf, A. J. Heeger, and G. C. Bazan, Improved high-efficiency organic solar cells via incorporation of a conjugated polyelectrolyte interlayer, J. Am. Chem. Soc. **133**, 8416 (2011).

[42] S. Chandran, N. Begam, V. Padmanabhan, and J. K. Basu, Confinement enhances dispersion in nanoparticlepolymer blend films, Nat. Commun. **5**, 4697 (2014).

[43] L. Meli, A. Arceo, and P. F. Green, Control of the entropic interactions and phase behavior of athermal nanoparticle/homopolymer thin film mixtures, Soft Matter **5**, 533 (2009).

[44] J. Kim and P. F. Green, Phase behavior of thin film brush-coated nanoparticles/homopolymer mixtures, Macromolecules **43**, 1524 (2010).

[45] J. Y. Lee, Z. Shou, and A. C. Balazs, Modeling the Self-Assembly of Copolymer-Nanoparticle Mixtures Confined between Solid Surfaces, Phys. Rev. Lett. **91**, 136103 (2003).

[46] V. Padmanabhan, A. L. Frischknecht, and M. E. Mackay, Effect of chain stiffness on nanoparticle segregation in polymer/nanoparticle blends near a substrate, Macromol. Theory Simul. **21**, 98 (2012).

[47] V. Padmanabhan, Effect of grafting on nanoparticle segregation in polymer/nanoparticle blends near a substrate, J. Chem. Phys. **137**, 094907 (2012).

[48] G. S. Grest and K. Kremer, Molecular dynamics simulation for polymers in the presence of a heat bath, Phys. Rev. A **33**, 3628 (1986).

[49] J. D. Weeks, D. Chandler, and H. C. Andersen, Role of repulsive forces in determining the equilibrium structure of simple liquids, J. Chem. Phys. **54**, 5237 (1971).

[50] See Supplemental Material at http://link.aps.org/supplemental/10.1103/PhysRevLett.114.258301, which includes Refs. [51–54], for simulation details and results of other grafting parameters considered in this study.

[51] S. Plimpton, Fast parallel algorithms for short-range molecular dynamics, J. Comput. Phys. **117**, 1 (1995).

[52] K. Kremer and G. S. Grest, Dynamics of entangled linear polymer melts: A molecular-dynamics simulation, J. Chem. Phys. **92**, 5057 (1990).

[53] M. A. Horsch, Z. Zhang, and S. C. Glotzer, Simulation studies of self-assembly of end-tethered nanorods in solution and role of rod aspect ratio and tether length, J. Chem. Phys. **125**, 184903 (2006).

[54] T. K. Patra and J. K. Singh, Polymer directed aggregation and dispersion of anisotropic nanoparticles, Soft Matter **10**, 1823 (2014).

[55] C. Chevigny, F. Dalmas, E. Di Cola, D. Gigmes, D. Bertin, F. Boue, and J. Jestin, Polymer-grafted-nanoparticles nanocomposites: Dispersion, grafted chain conformation, and rheological behavior, Macromolecules **44**, 122 (2011).